AIP | The Journal of Chemical Physics

Matrix isolation studies of the reactions of silicon atoms. I. Interaction with water: The infrared spectrum of hydroxysilylene HSiOH

Zakya Kafafi Ismail, Robert H. Hauge, Leif Fredin, James W. Kauffman, and John L. Margrave

Citation: The Journal of Chemical Physics **77**, 1617 (1982); doi: 10.1063/1.444082
View online: http://dx.doi.org/10.1063/1.444082
View Table of Contents: http://scitation.aip.org/content/aip/journal/jcp/77/4?ver=pdfcov
Published by the AIP Publishing

Matrix isolation studies of the reactions of silicon atoms: I. Interaction with water: The infrared spectrum of hydroxysilylene HSiOH

Zakya Kafafi Ismail, Robert H. Hauge, Leif Fredin, James W. Kauffman, and John L. Margrave

Department of Chemistry and the Rice Quantum Institute, Rice University, Houston, Texas 77251

(Received 15 February 1982; accepted 16 April 1982)

This study focuses on the interactions and reactions of silicon atoms and molecules with water. Initially, a silicon–water adduct ($Si{:}OH_2$) is formed, as noticed from the red shift of the ν_2 bending modes of H_2O, HDO, and D_2O. This silicon "hydrate" complex rearranges spontaneously through hydrogen tunneling to give HSiOH and HSiOD as final products of the reaction of Si with H_2O and HDO. Photolysis of $Si{:}OD_2$ with $\lambda \geq 400$ nm is necessary for the production of the deuterated insertion product DSiOD. All silicon hydroxy–hydrides undergo a photolytic decomposition reaction when strongly irradiated to give silicon monoxide and molecular hydrogen or two hydrogen atoms. Band assignments for *trans*-HSiOH, *trans*- and *cis*-HSiOD, and DSiOD have been made. It appears that the *cis*-isomer converts to the more stable *trans*-isomer when the matrix is heated. The SiOH bond angle has been calculated for a planar structure of C_s symmetry using the Redlich–Teller product rule and the torsional frequencies for HSiOH, HSiOD, and DSiOD. Normal coordinate analyses have been carried out using the measured frequencies for six isotopomers, namely, HSiOH, HSiOD, DSiOD, $HSi\,^{18}OH$, $HSi\,^{18}OD$, and $DSi\,^{18}OD$. Thermodynamic properties have also been calculated for this new species.

I. INTRODUCTION

In the past few years, theoretical[1–7] and experimental[8–13] studies have revealed the existence of a novel group of molecular complexes between metal atoms and classical Lewis bases such as H_2O, HF, NH_3, and H_2S. The bonding in these complexes is the result of charge transfer from the negative end of the hydride to the metal. In the reactions of metals with water for instance, H_2O serves as an electron donor through its $3a_1$ orbital. The interaction is stabilized by polarization of electron density on the metal away from the oxygen. Most of these metal complexes, except for the Group IA, undergo rearrangement with or without appreciable energy barriers to form the insertion products HMOH (where M = metal). Sc, Ti, V, and Al are examples of metals that spontaneously insert into the OH bond of water.[13]

A number of interesting products can form in silicon-water reactions. Table I shows estimated heats of reactions for various possible products based on JANAF table bond energies. As seen from this table, all reactions are exothermic; hence, one might expect the formation of one or more of these products when silicon atoms are cocondensed with water in solid argon.

The present paper deals with a study of the interactions of silicon atoms and molecules with water in solid argon (15 K). This investigation may help provide a better understanding of surface–water reactions of ultrapure silicon as well as the formation of water-induced thin film impurities, which occur in the preparation of ultrapure semiconductor materials in the electronics industry. This work may also help in the elucidation of mechanisms for reactions that involve the insertion of a silicon atom into an OH bond.

II. EXPERIMENTAL

The matrix isolation apparatus has been fully described by Ismail[16] and Kauffman.[13] An Air Products Displex closed cycle refrigerator, model CSW-202 has been used in all matrix experiments. Matheson argon (99.99%) was further purified by passing it through hot titanium (900 °C) prior to deposition. Silicon (>99%) obtained from MCB was used without further purification. Deionized water was the source of $H_2{}^{16}O$. D_2O (98.8%) and $H_2{}^{18}O$ (95%) were purchased from Columbia Organic Chemicals Co. and Prochem Isotopes, respectively. All dissolved gases in water were eliminated through several freeze–vacuum thaw cycles. A quartz crystal was mounted on one of the polished copper surfaces in good thermal contact with the cold block. The rates of deposition of silicon, water, and argon were measured by determining the frequency change of the crystal oscillator. The flow rate of water was usually adjusted by a leak valve and monitored by a thermocouple gauge. Readings in the range of ~100–150 μ were typical. Silicon was vaporized from a high density graphite crucible over the temperature range 1450–1650 °C which corresponds to vapor pressures of 1×10^{-3}–1×10^{-2} mm Hg. The furnace was slightly tilted in order to prevent liquid silicon from running out of the cell and reacting with the tantalum heater. The temperature of the graphite crucible was measured with an optical pyrometer.

TABLE I. Estimated heats of reaction for $Si + H_2O$ to yield various products.

Product	ΔH (kcal/mol)
$Si \cdots OH_2$	-5 ± 5
$HSiOH^a$	-58 ± 15
$SiO + H_2$	-76 ± 2
H_2SiO^b	-72 ± 15

[a] Assuming B.E. (SiH) ≃ 76 kcal/mol (Ref. 14) and B.E.(Si–OH) ≃ B.E.(Si–Cl) = 102 kcal/mol.

[b] Assumes value of $H_2SiO \rightarrow H_2Si(^1A) + O(^3P)$ of +140 kcal/mol (Ref. 15).

0021-9606/82/161617-09$02.10

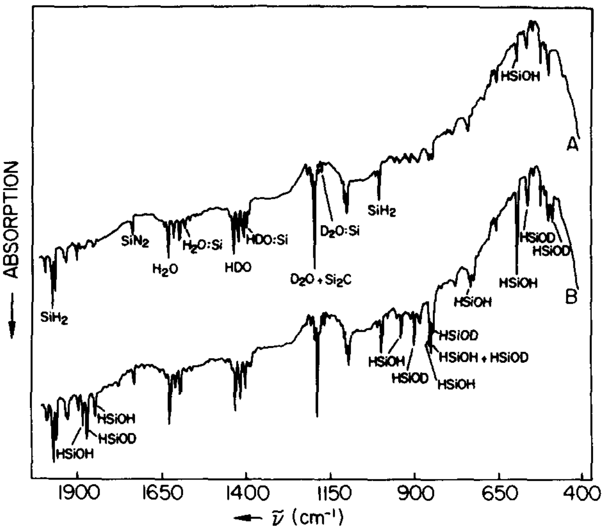

A & B = Spectra measured immediately and 7 hours after trapping

FIG. 1. Infrared spectra of products from the reaction of silicon with H_2O/D_2O in solid argon. Spectrum A was recorded immediately after trapping and spectrum B was measured 7 h later. (Note that the matrix was protected from Nernst glower radiation by keeping the shutter closed; however, leaving the shutter open did not have any effect on the matrix.)

Spectra of trapped pure silicon showed the presence of bands due to monosilane (SiH_4) and silylene (SiH_2) which are the result of reactions of silicon atoms with molecular hydrogen on the matrix surface.[17,18] The hydrogen impurity probably results from cracking of the organic pump oil. Passing liquid nitrogen rather than water through the copper heat shield surrounding the furnace considerably reduced the amount of SiH_4 and SiH_2. Some Si_2C was also present as an impurity as a result of the reaction of Si with the graphite crucible.[19] In some experiments a very small amount of nitrogen was present due to the development of a temporary minor leak in the system. This impurity was detected by the absorption band due to SiN_2.[20] (See Fig. 1.)

Matrices were usually irradiated subsequent to deposition. The radiation source used was a 100 W medium pressure short arc mercury lamp which was focused to a 2 cm diameter spot on the matrix surface. A water/Pyrex filter with various Corning long-pass cutoff filters was used for wavelength dependent photolysis studies.

Annealing of the matrices was carried out in some experiments to eliminate unstable matrix sites and to help identify certain bands. It usually involved doubling the temperature of the matrix for a short period of time and then cooling it back again to its original temperature (~ 15 K).

Infrared reflection spectra were recorded with a Beckman IR-9 spectrometer. All spectra were calibrated against known H_2O and NH_3 lines in the different infrared regions. Frequencies were measured to an accuracy of ± 0.5 cm^{-1}.

III. RESULTS

Cocondensation of silicon and water in excess argon at 15 K gave an orange-yellow matrix. The infrared spectrum measured immediately after deposition of silicon and a mixture of H_2O/D_2O in excess argon is shown in Fig. 1A. The ratio of silicon to water and argon was 9 : 1 : 3300 and represents one of the highest concentrations of silicon used. Three new bands were observed in the ν_2 bending regions of H_2O, HDO, and D_2O at 1574.7, 1389.7, and 1163.3 cm^{-1}, respectively. They have been assigned to the silicon-water adduct molecules: $Si:OH_2$, Si : OHD, and $Si:OD_2$. Table II compares the measured frequencies for the 0_0–0_0 ν_2 transition of water isotopomers and their red-shifted analogs for the silicon-water adducts. This shift has been successfully used as a semiquantitative measure of the strength of the interaction between various metal atoms and the water molecule.

The set of three bands at the low frequency end of the spectrum was only present under high concentrations of silicon. Thus, they were associated with reaction products of silicon molecules or higher aggregates with water.

Figure 1B shows the same spectrum measured 7 h later. It is interesting to note the striking changes that have occurred in the spectrum by leaving the trapped species in the dark at 15 K for several hours. The intensities of the $H_2O:Si$ and HDO : Si bands have considerably decreased. New bands appear in the O–H (in case of H_2O), Si–H, and Si–O stretching regions as well as in other regions. From the different absorption regions of these bands and from the isotopic shifts, one can conclude that the silicon water adduct rearranged and formed the insertion product HSiOH. Assuming that HSiOH is planar, one expects to observe six infrared active modes: five in-plane modes and one out-of-plane mode. The five in-plane modes may essentially be classified as three stretching modes (O–H, Si–H, and Si–O) and two bending modes (HSiO and SiOH). Finally, an out-of-plane mode which is due to torsion of the two hydrogens about the Si–O bond should give rise to the sixth absorption band. The bands at 850.6 and 840.5 cm^{-1} show a considerable isotope shift upon oxygen-18 substitution. They have been assigned to the Si–O stretching modes of HSiOH and HSiOD, respectively. The absorption at 937.0 cm^{-1} shows a small shift in case of HSiOD but a very large one in case of DSiOD. It is reasonable to assign this band to the HSiO bending mode. The first overtone of this bending mode interacts with the Si–H stretching mode and causes the splitting of the bands near 1900 cm^{-1}. This is an example of a Fermi resonance interaction which is not seen in case of HSiOD because of the lower frequency of the HSiO bending mode. The Si–H absorption occurs at 1872.3

TABLE II. Comparison between measured frequencies (cm^{-1}) for the water bending mode and their shifted analogs for the silicon water adduct.

H_2O	HDO	D_2O	$H_2{}^{18}O$	$HD^{18}O$	$D_2{}^{18}O$
1593.0	1402.1	1177.0	1586.9	1394.6	1169.5
1574.7	1389.7	1168.3	1568.2	1382.0	1158.6
H_2O: Si	HDO: Si	D_2O: Si	$H_2{}^{18}O$: Si	$HD^{18}O$: Si	$D_2{}^{18}O$: Si

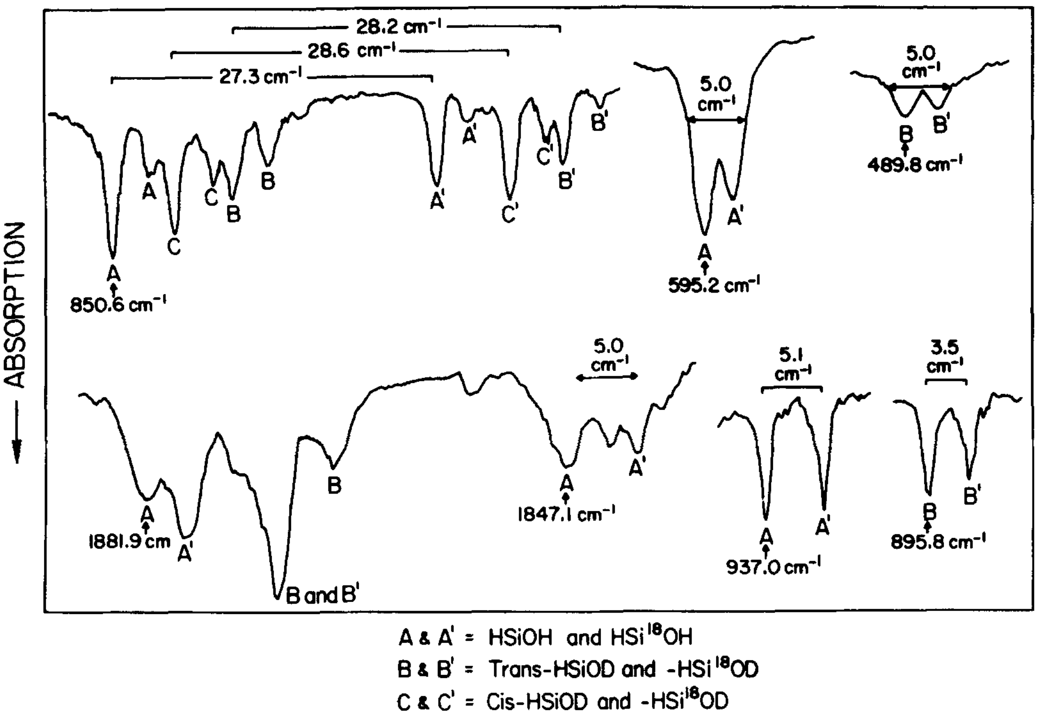

FIG. 2. Expanded high resolution infrared spectra of the different absorption regions of HSiOH, HSi ^{18}OH, *trans*- and *cis*- HSiOD, and HSi ^{18}OD A and A' = HSiOH and HSi ^{18}OH, B and B' = *trans*- HSiOD and HSi ^{18}OD, and C and C' = *cis*- HSiOD and HSi ^{18}OD. Ratio of Si to Ar is 1 : 1000. Ratio of Si to H_2 $^{18}O/D_2O$ is 5 : 4. The intensity of the peak at 595.2 cm^{-1} represents a 30% absorption.

cm^{-1} for HSiOD. There are two other bands associated with HSiOH, namely at 722.6 and 595.2 cm^{-1}, respectively. One of those absorptions must be due to the SiOH bending mode and the other is related to the torsional mode. The band with lowest frequency has been assigned to the out-of-plane mode. This assignment has been verified through use of the product rule.

Figure 2 shows an expanded spectrum of the different absorption regions of HSiOH, HSi ^{18}OH, HSiOD, and HSi ^{18}OD. It is interesting to note that in case of HSiOD, one is able to observe absorption peaks that can be assigned to both *trans*- and *cis*- isomers. On the other hand, only bands of the most stable isomer of HSiOH are detected. The *trans*-isomer has been assumed to be the more stable isomer (see the Discussion Sec.). This unusual behavior may be explained by the fact that the zero point energy for the partially deuterated *cis*- and *trans*-HSiOD is lower than that of *cis*- and *trans*-HSiOH. Thus, the *cis*- isomer of HSiOD is trapped in a shallow potential energy well while that for HSiOH is not.

Figure 3 shows a spectrum when silicon atoms are codeposited with D_2O in argon. Unlike the reactions of H_2O and HDO with Si, D_2O only forms the adduct Si : OD_2 upon interaction with silicon. Photolysis with a medium pressure mercury lamp is necessary for the production of the deuterated insertion product DSiOD. Again bands associated with *cis*- and *trans*-DSiOD are observed. The Si–D stretching mode shows an absorption at 1354.5 cm^{-1}.

Table III lists the measured infrared frequencies for all of the predominant bands for *trans*- HSiOH, HSiOD, and DSiOD. It is interesting to note that upon oxygen-18 substitution, the D–Si stretch shifts upward by 7.7 cm^{-1}. The only plausible explanation for this positive shift is that there is a Fermi resonance interaction between the Si–D mode and a combination band of ν_4 (SiO) and the unobserved ν_5 (SiOD). This is a particularly significant observation since this unusual shift verifies the position of the SiOD bending mode and confirms the assignment of the out-of-plane torsional mode. The

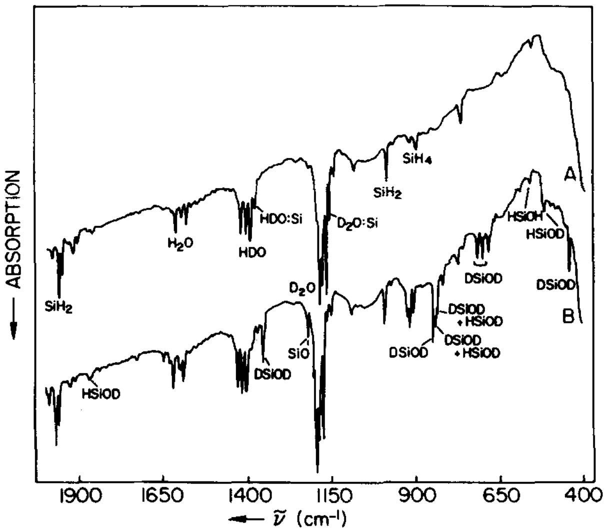

FIG. 3. Infrared spectra of products from the reaction of silicon with D_2O in solid argon. Spectrum A was measured immediately after deposition and spectrum B was recorded after photolysis (~ 20 s) with a short arc Hg lamp.

TABLE III. Infrared frequencies (cm^{-1}) for the isotopomers[a] of silicon hydroxy–hydrides in Ar matrices.

Vibrational mode	HSiOH	HSiOD	DSiOD	HSi^{18}OH	HSi^{18}OD	DSi^{18}OD
ν_1 (H–O)	3650.0					
ν_2 (H–Si)	1881.9, 1847.1	1872.3	1354.5	1880.0, 1841.8	1872.0	1362.2
ν_3 (HSiO)	937.0	895.8	715.1	932.1	892.3	706.2
ν_4 (Si–O)	850.6	840.5	840.7	823.1	812.1	812.3
ν_5 (SiOH)	722.6	563.2	521.2	720.0	560.5	
ν_6 (torsion)	595.2	489.8	447.3	593.6	486.9	444.0

[a] All predominant bands and bands associated with the *trans*-isomer in case of the totally and partially deuterated species.

out-of-plane mode belongs to a symmetry class (A'') of its own and is not allowed to interact with any of the other modes (symmetry A'). Thus, the mode assignments for all bands have been verified.

Table IV compares the measured frequencies for *cis*- and *trans*- HSiOD and DSiOD as well as HSi^{18}OD and DSi^{18}OD. In all cases, the O–H and the O–D stretching frequencies were not observed. This could be due to their being too weak to be observed or simply being overlapped by the OH and OD bands of HDO and D_2O, respectively. The HSi and DSi stretching frequencies are the same for *cis*- and *trans*- isomers. They have been listed in the previous table. The torsional frequency also appears to be the same for the *cis*- and *trans*- isomers. This coincidence is suggested by annealing experiments. Annealing causes conversion of the *cis*- isomer to the more stable *trans*- isomer, as shown by a decrease in the intensity of the *cis*- bands and an increase in the intensity of the *trans*- bands. However, the intensity of the assigned torsional mode is unchanged as would be expected if this mode occurs at the same frequency for both isomers. The HSiO bending frequency is lower for the *cis*- than the *trans*-form but a reverse effect is observed for the SiO stretching frequency. Also, the isotopic frequency shifts are considerably different for *cis*- and *trans*- HSiOD and DSiOD. For the SiOH bending mode of the above only absorption bands associated with the *trans*- isomers are observed. They are relatively weak absorptions which probably accounts for the failure to observe these bands for the less predominant *cis*- isomers.

IV. DISCUSSION

A. Reaction of silicon with water

1. H_2O

From the above experimental results, it is seen that silicon atoms initially react with H_2O to form the adduct Si : OH_2. This silicon–water complex slowly rearranges to form the insertion product HSiOH. Irradiation of the matrix with light from a short arc mercury lamp causes the dissociation of the divalent silicon hydroxy–hydride and the formation of silicon monoxide and molecular hydrogen or two hydrogen atoms. In the presence of excess water, the hydrated insertion product HSiOH : H_2O is also formed. When exposed to the light from the mercury lamp, it is photolyzed to yield dihydroxysilane $H_2Si(OH)_2$.

2. HDO

Similar to H_2O, HDO initially reacts with Si atoms to give the adduct Si : OHD. Once the adduct is formed, silicon can theoretically insert in the OH bond and/or in the OD bond. Experiment shows that only insertion into the OH bond takes place. Attempts to produce DSiOH through careful photolysis of the adduct Si : OHD proved in vain. It seems that silicon strongly prefers to insert in the OH rather than the OD bond when both bonds are available. This behavior is an interesting manifestation of the hydrogen–deuterium isotope effect. One also observes formation of both the *cis*- and *trans*- isomers of the insertion product. This is apparently due to the fact that the zero point energy for *cis*- HSiOD is lower than for *cis*- HSiOH. Once HSiOD is formed, it can be photolyzed to give SiO and HD or H and D. In excess HDO, reactions similar to those described for H_2O take place.

3. D_2O

Unlike their reactions with H_2O and HDO, the reaction of Si atoms with D_2O proceeds spontaneously no farther than to form the adduct Si : OD_2. Photolysis of the matrix with light ($\lambda \geq 400$ nm) is necessary for the formation of DSiOD. DSiOD will also dissociate upon strong irradiation to yield SiO and D_2 or 2D. In the presence of high concentrations of D_2O, similar reac-

TABLE IV. Measured infrared frequencies for *cis*- and *trans*-HSiOD, HSi^{18}OD, DSiOD, and DSi^{18}OD.

Vibrational mode	HSiOD		DSiOD		HSi^{18}OD		DSi^{18}OD	
	cis	*trans*	*cis*	*trans*	*cis*	*trans*	*cis*	*trans*
ν_3 (HSiO)	881.4	895.8	700.7	715.1	877.9	892.3	695.3	706.2
ν_4 (SiO)	845.4	840.5	847.0	840.7	816.7	812.1	820.9	812.3
ν_5 (SiOH)	⋯	563.2	⋯	521.2	⋯	560.5	⋯	⋯

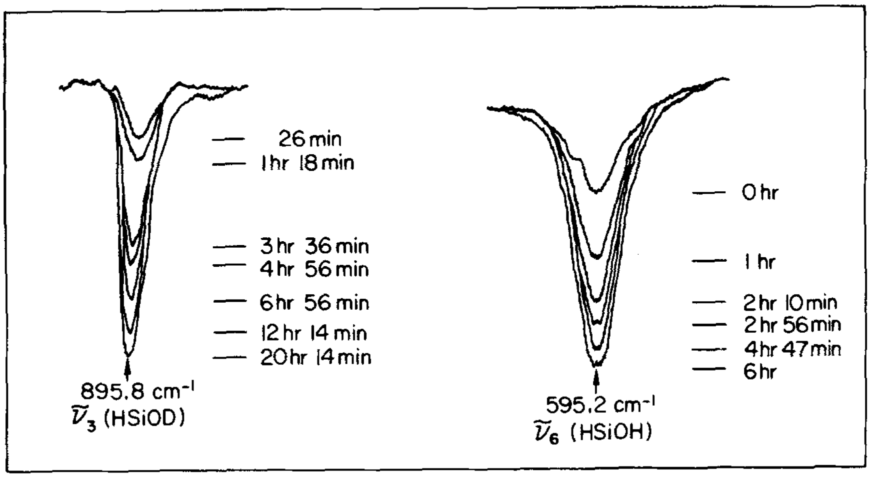

FIG. 4. Relationship between the $\tilde{\nu}_6$ (HSiOH) and $\tilde{\nu}_3$ (HSiOD) bands and time.

tions to those of H_2O and HDO take place, giving the final product $D_2Si(OD)_2$.

B. Hydrogen tunneling

It has been noted that the insertion products, HSiOH and HSiOD slowly form in the dark in a matrix at 15 K during the first few hours after deposition. On the other hand, photoexcitation of the adduct $Si:OD_2$ was necessary for the formation of the insertion product DSiOD. Figure 4 shows the growth of the ν_6 (HSiOH) and the ν_3 (HSiOD) bands as a function of time. The HSiOH peak stopped growing after 6 h. It took the HSiOD band almost 20 h before it reached its maximum height. Assuming that the following unimolecular reaction is taking place:

$$Si:OH_2 \rightarrow HSiOH$$

one can derive the following rate law for this reaction

$$-\log|[\mathrm{HSiOH}]_\infty - [\mathrm{HSiOH}]| = kt - \log[\mathrm{HSiOH}]_\infty ,$$

where k = rate constant, t = time, and [HSiOH] = concentration of HSiOH. Figure 5 gives a plot of the rates of formation of HSiOH and HSiOD in terms of their absorbance (α concentration). It is clear from the slopes of the two curves that the rates of formation of HSiOH and HSiOD are quite different. The ratio of the relative rate constants for HSiOH/HSiOD is about four. Raising the temperature of the matrix did not affect the reaction rates. Hence, this behavior cannot be explained in terms of a classical isotope effect. The most plausible explanation for this phenomenon is that hydrogen tunneling is involved in the process of formation of HSiOH and HSiOD. In the case of the reaction to form DSiOD, tunneling is apparently too slow to be observed.

C. Fermi resonance interaction

A Fermi interaction between the Si–H stretching frequency and the HSiO bending mode occurs for HSiOH and $HSi^{18}OH$. If one assumes that the unperturbed Si–H stretching frequency for HSiOH is the same as that for HSiOD, one can calculate the magnitude of the Fermi interaction and the anharmonicity of the HSiO bending mode. One calculates a Fermi interaction of 9.6 and 8.0 cm^{-1} for HSiOH and $HSi^{18}OH$, respectively, between the Si–H stretching mode and the first overtone of the HSiO bending mode. One also calculates an anharmonicity of 17.3 and 14.4 cm^{-1}, respectively, for the HSiO bending modes of HSiOH and $HSi^{18}OH$. An average value of 15.9 cm^{-1} for the anharmonic correction for the HSiO bending mode seems quite reasonable. There is a Fermi interaction between the D–Si stretching mode of $DSi^{18}OD$ and a combination band of ν_4 (Si–O) and ν_5 (SiOD). Assuming that the unperturbed D–Si stretching frequency for $DSi^{18}OD$ is the same as that of DSiOD, one calculates a Fermi interaction of 7.7 cm^{-1}. This interaction is the cause for the observed blue shift in ν_2 (D–Si) upon ^{18}O substitution in DSiOD.

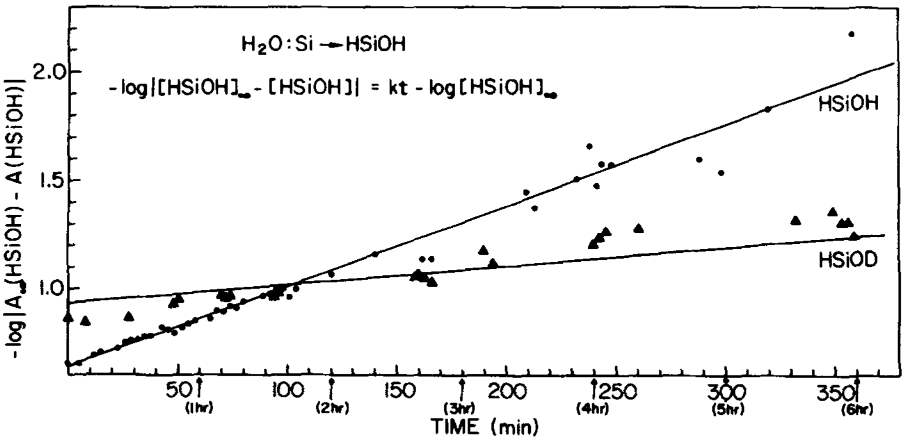

FIG. 5. Rates of formation of HSiOH and HSiOD. (Note that the rate of formation of HSiOD has been measured over a period of ~20 h.)

D. Geometry of HSiOH

Jordan[21] has carried out SCF calculations using a 321G basis set which consists of *s* and *p* functions on HMOH (where M = Be, B, C, Mg, Al, and Si) molecules. His theoretical study suggests that HSiOH should exist in both *cis*- and *trans*- planar forms. The energies of the *cis*- and *trans*- structures are predicted to be very close but tend to favor the *trans*- isomer slightly. For *trans*- HSiOH, values of 95.6° and 122.9° have been calculated for HSiO and SiOH bond angles, respectively, with the following values for bond distances: $r_{\mathrm{HSi}} = 1.525$ Å, $r_{\mathrm{SiO}} = 1.675$ Å, and $r_{\mathrm{OH}} = 0.962$ Å. *Ab initio* calculations[22] on HCOH have shown that the *trans*- isomer is more stable by 4.9 kcal/mol than the *cis*- isomer. The following geometry has been calculated for *trans*- HCOH: $r_{\mathrm{CH}} = 1.113$ Å, $r_{\mathrm{CO}} = 1.323$ Å, and $R_{\mathrm{OH}} = 0.978$ Å, HCO = 101.4°, and COH = 107.2°.

Walsh[23] has discovered and, later Gimarc[24] has shown that it is possible to predict and explain the molecular structure of simple polyatomic molecules as a function of the number of valence electrons. N_2H_2 has been predicted to exist as planar *cis*- or *trans*- forms. It has been experimentally observed in its *trans*- planar form.[25] By analogy to N_2H_2, which has the same number of valence electrons as HSiOH and based on the above mentioned theoretical calculations the proposed lowest energy structure for HSiOH is *trans*- planar of C_s symmetry. This planarity might also be predicted by the fact that one expects partial π back-bonding between the filled *p* orbitals of oxygen and the empty *p* orbitals of silicon.

Bond lengths for HSiOH have been transferred from those of SiH_2 (SiH), SiF_2 (SiF = SiO), and H_2O (OH), respectively. It seems quite reasonable to assume that the Si–OH distance is about the same as that of Si–F since it is known[26,27] that the properties of Si–OH and Si–F bonds are closely similar. The HSiO bond angle has been taken to be the average of the HSiH and FSiF bond angles.

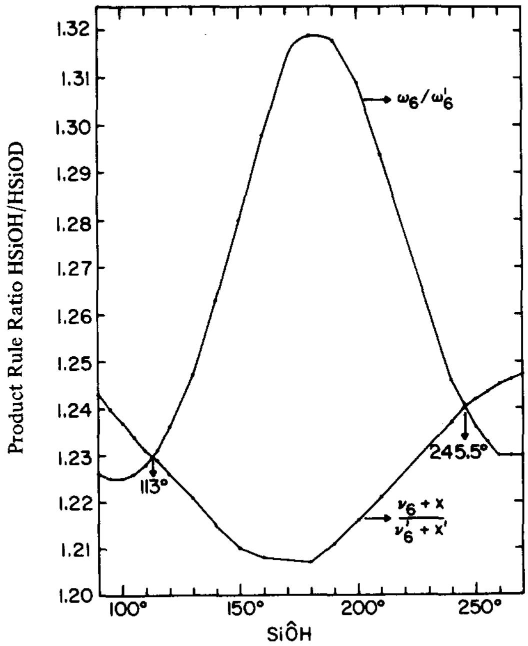

FIG. 6. Theoretical and adjusted experimental product rule for HSiOH/HSiOD (vertical axis) vs SiOH angle.

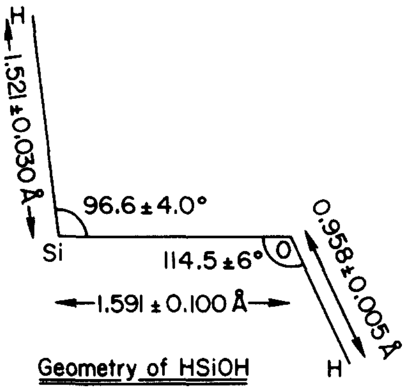

FIG. 7. Proposed geometry for HSiOH. All geometrical parameters are estimated except the SiOH bond angle.

Taking advantage of the fact that the torsional mode belongs to a symmetry class (A'') of its own, one is able to calculate the SiOH bond angle quite accurately from the Teller–Redlich product rule which has the following form:

$$\frac{w_6}{w_6^i} = \left(\frac{m_{\mathrm{Si}}^i}{m_{\mathrm{Si}}}\right)^{1/2} \left(\frac{m_{\mathrm{O}}^i}{m_{\mathrm{O}}}\right)^{1/2} \left(\frac{M}{M^i}\right)^{1/2} \left(\frac{I_x I_y}{I_x^i I_y^i}\right)^{1/2},$$

where w_6 = harmonic torsional frequency, i = isotope, m_{H}, m_{Si}, m_{O} = masses of hydrogen, silicon, and oxygen, respectively, M = molecular weight of HSiOH, and I_x, I_y = moments of inertia about principal axes x and y (x and y lie in the plane of the molecule).

In order to reach the desired level of accuracy in the calculated bond angle, one has to make a correction for anharmonicity in the measured frequency of the torsional mode. A derived anharmonicity x is obtained by calculating the product rule w_6/w_6^i for a particular set of isotopomers. In our case, we have used HSiOH/DSiOD with the above equation for different values of the SiOH angle. The right-hand side of the above equation is equated to $(\nu_6 + x)/\nu_6^i + x^i)$, where ν_6 = observed frequency and $x^i = (\nu_6^i/\nu_6)^2 x$. From the above relationship, it is clear that the derived anharmonicity will vary with the SiOH angle. This anharmonicity is then used to give an adjusted experimental ratio for the product rule of HSiOH/HSiOD for each value of the SiOH bond angle. Plotting the adjusted experimental and theoretical product rules as a function of angle gives rise to the curves in Fig. 6. These two curves intersect at two points, indicating the value of SiOH = 113° for the *cis*- isomer and SiÔH = 114.5° for the *trans*- isomer. An anharmonicity equal to 75.5 cm^{-1} corresponds to the calculated angle for *trans*- HSiOH which is also indicated by the point of intersection. If one assumes that the ratio of anharmonicities is proportional to the ratio of the G matrices, an improved value of x is calculated to be 63.9 cm^{-1}. Figure 7 shows the predicted geometry of *trans*- HSiOH which is the isomer that was experimentally observed. Errors in these calculations arise from uncertainties in the measured frequencies (± 0.5 cm^{-1}) and estimated geometrical parameters, and from the assumption that the ratio of anharmonicities is proportional to the ratio of the G matrices for this

TABLE V. Harmonic force constants for *trans*-HSiOH (C_s symmetry).

Force constant[a]	Value
k (H–Si)	2.007
k (Si–O)	4.463
k (O–H)	7.435
k (HSiO)	0.930
k (SiOH)	0.324
k (torsion)	0.137
k (HSiO, SiO)	0.390
k (SiOH, SiO)	0.152
k (HSiO, SiOH)	0.100

[a] Stretching constants in mdyn/Å; bending constants in mdyn Å/rad^2 and stretch–bend interaction constants in mdyn/rad.

mode. It is worth pointing out that an error in the assumed H$\hat{\mathrm{Si}}$O bond angle will give rise to an error of the same order of magnitude in the Si$\hat{\mathrm{O}}$H angle. It is reasonable to assume that 96.6° is the lower limit value for H$\hat{\mathrm{Si}}$O and hence the Si$\hat{\mathrm{O}}$H bond angle is not smaller than 114.5°. An upper limit value of 100° in a H$\hat{\mathrm{Si}}$O angle would correspond to an increase in the Si$\hat{\mathrm{O}}$H bond angle of ~3°. The SiOH bond angle is not equally affected by similar changes in each of the three bond lengths. Increasing the SiO bond by 0.1 Å does not cause any deviation in the calculated value of the SiOH bond angle. However, a 10% increase in the OH bond length will cause a 21% decrease in the SiOH bond angle. Lengthening the SiH bond by 0.15 Å will have an opposite effect on the SiOH bond angle, namely, an increase of 12.8°. Estimates of the OH and SiH bond lengths should be accurate to within 0.005 and 0.03 Å, respectively, which will introduce an uncertainty of ±3° in the calculated bond angle. It is more difficult to estimate the SiO bond length (assumed to be equal to that of SiF). Comparing the estimated value for SiO with that calculated by Jordan[21] one should not expect an uncertainty higher than ±0.1 Å. This uncertainty has no effect on the calculated bond angle. Thus, one concludes that the SiOH bond angle is 114.5±6°. It should be pointed out that if frequencies for different sets of isotopomers are used in the calculations, one arrives at the same value for the calculated bond angle and anharmonicity.

E. Normal coordinate analysis

Using the calculated geometry for HSiOH and assuming the force constants listed in Table V, one can calculate frequencies for all HSiOH isotopomers and compare them with measured ones. A normal coordinate analysis program written by Schachtsneider[28] has been used in this calculation. The initial values for the Si–H, Si–O, O–H, and HSiO force constants have been transferred from known force constants for SiH_2[18] (k_{SiH}), SiF_2[29] ($K_{SiF} = k_{SiO}$), H_2O[30] (k_{OH}), and HSiF[27] (k_{HSiF}). The effects of individual interaction force constants on calculated frequencies and isotopic shifts were tested. All stretch–stretch interaction force constants as well as stretch–bend (SiH/OH with HSiO/SiOH) interaction force constants appear to be appreciably less important than those listed in Table V and were assumed to be zero in the final calculations. With the minimum number of interaction force constants, a perturbation cycle was carried out until the best fit to the observed frequencies was achieved. Table VI compares measured and calculated frequencies for HSiOH and all of its isotopomers. One notices the general good agreement between these sets of values considering the assumption of harmonic frequencies. The agreement for the torsional frequency is much better since it was corrected for anharmonicity and is of different symmetry than the other five modes.

F. Thermodynamic properties of HSiOH

Although the molecule HSiOH has been observed for the first time in solid argon matrices, there is also the possibility that it may be present in the gas phase under proper conditions. Table VII lists gas phase thermodynamic functions over the range 298.15–5000 K based upon the inertial product 11.61×10^{-117} gm^3 cm^6, the harmonic oscillator approximation, and vibrational frequencies of the isotopic molecule most prevalent in natural abundance.

G. Reaction pathways

A diagram of the energy levels of the products HSiOH, SiO, and H_2 relative to that of the reactants Si and H_2O is shown in Fig. 8. A comparison of the relative positions of excited states of two of the possible products may explain the formation of the less stable HSiOH rather than SiO and H_2. Conservation of spin suggests that the HSiOH product is the only one which has a triplet state that may be accessed from the initial reactant

TABLE VI. Comparison between observed and calculated frequencies (cm^{-1}) of *trans*-HSiOH and all of its isotopomers.[a]

Vibrational mode	HSiOH		HSiOD		DSiOD		HSi^{18}OH		HSi^{18}OD		DSi^{18}OD	
	Obs.	Calc.	Obs.	Calc.	Obs.	Calc.	Obs.	Calc.	Obs.	Calc.	Obs.	Calc.
ν_1 (OH)	3650.0	3650.7	···	2660.6	···	2660.5	···	3638.4	···	2643.3	···	2643.2
ν_2 (SiH)	1872.3[b]	1872.3	1872.3	1872.3	1354.5	1348.4	1872.0[b]	1872.3	1872.0	1872.3	1354.2[b]	1348.4
ν_3 (HSiO)	937.0	940.5	895.8	896.0	715.1	706.3	932.1	935.6	892.3	891.2	706.2	700.5
ν_4 (SiO)	850.6	852.0	840.5	840.3	840.7	842.2	823.1	821.6	812.1	811.1	812.3	811.8
ν_5 (SiOH)	722.6	721.5	563.2	561.4	521.2	525.3	720.0	720.8	560.5	559.7	···	524.8
ν_6 (torsion)	659.1	659.2	531.2	531.2	481.2	481.5	657.0	656.9	527.6	528.4	477.2	478.3

[a] All observed torsional frequencies have been corrected for anharmonicities.
[b] Unperturbed frequencies (observed for HSiOD, HSi^{18}OD, and DSiOD).

TABLE VII. Ideal gas functions for *trans*-HSiOH.[a]

Temp. (K)	C_p° (cal/mol K)	$(H_T^\circ - H_0^\circ)/T$ (kcal/mol K)	$H_T^\circ - H_{298}^\circ$ (kcal/mol)	$\frac{-(G_T^\circ - H_0^\circ)}{T}$ (cal/mol K)	$\frac{-(G_T^\circ - H_{298}^\circ)}{T}$ (cal/mol K)	S_T° (cal/mol K)
298.15	10.663	8.668	0.000	47.657	56.325	56.325
300	10.696	8.680	0.020	47.710	56.325	56.391
400	12.264	9.389	1.171	50.304	56.764	59.692
500	13.449	10.088	2.460	52.475	57.643	62.563
600	14.345	10.726	3.851	54.371	58.679	65.097
700	15.046	11.295	5.322	56.068	59.760	67.363
800	15.613	11.801	6.856	57.610	60.841	69.411
900	16.085	12.251	8.442	59.027	61.898	71.278
1000	16.486	12.655	10.071	60.339	62.923	72.994
1100	16.832	13.020	11.737	61.562	63.912	74.582
1200	17.132	13.350	13.436	62.710	64.863	76.060
1300	17.394	13.651	15.162	63.790	65.778	77.441
1400	17.625	13.927	16.913	64.812	66.658	78.739
1500	17.828	14.180	18.686	65.782	67.505	79.962
1600	18.007	14.414	20.478	66.704	68.320	81.119
1700	18.166	14.630	22.287	67.585	69.105	82.215
1800	18.307	14.831	24.111	68.427	69.863	83.258
1900	18.433	15.017	25.948	69.234	70.594	84.251
2000	18.545	15.191	27.797	70.009	71.301	85.199
2100	18.646	15.353	29.657	70.754	71.984	86.107
2200	18.736	15.505	31.526	71.471	72.646	86.976
2300	18.817	15.647	33.404	72.164	73.287	87.811
2400	18.890	15.781	35.289	72.833	73.909	88.613
2500	18.957	15.906	37.181	73.479	74.513	89.386
2600	19.017	16.025	39.080	74.106	75.100	90.130
2700	19.071	16.137	40.985	74.712	75.670	90.849
2800	19.121	16.242	42.894	75.301	76.224	91.544
2900	19.166	16.342	44.809	75.873	76.764	92.215
3000	19.208	16.437	46.727	76.429	77.290	92.866
3200	19.281	16.613	50.576	77.495	78.303	94.108
3400	19.343	16.772	54.439	78.507	79.267	95.279
3600	19.396	16.916	58.313	79.470	80.188	96.386
3800	19.442	17.048	62.197	80.388	81.068	97.436
4000	19.481	17.168	66.089	81.266	81.912	98.434
4500	19.559	17.430	75.850	83.303	83.878	100.733
5000	19.616	17.646	85.645	85.151	85.668	102.797

[a] Normal isotopic abundancies.

states. The lowest lying triplet state of H_2SiO is also expected to be as high if not higher than that for SiO; however, this is not shown in Fig. 8. The following description is presented as a reasonable interpretation of the silicon atom/water reaction. Silicon in its triplet ground state reacts with water to form the $Si:OH_2$ adduct which slowly converts to the HSiOH insertion product. In order to preserve the spin multiplicity, HSiOH must initially be formed in its triplet excited state about 18 600 cm^{-1} higher than the ground state. This estimated difference between the triplet and the singlet states was calculated assuming that the interaction between Si and O in the adduct is about 5 kcal/mol. HSiOH* then decays to its ground singlet state. Upon exposure to light of $\lambda \geq 400$ nm, HSiOH is initially excited to its first singlet excited state. It then predissociates to silicon monoxide and molecular hydrogen or hydrogen atoms.

V. CONCLUSIONS

(1) This study has shown that the following reactions take place when Si atoms are cocondensed with H_2O in excess argon: $Si(^3P) + H_2O \rightarrow Si \cdots OH_2\ (^3A_2) \rightarrow HSiOH^*\ (^3A'') \rightarrow HSiOH\ (^1A') \xrightarrow{h\nu} SiO\ (^1\Sigma^+) + H_2\ (^1\Sigma_g^+)$ or possibly 2H. In the presence of excess H_2O, one also observes the following reactions which will be discussed in more detail in a further publication: $Si + H_2O \rightarrow Si \cdots (OH_2)_2 \rightarrow HSiOH \cdot H_2O \xrightarrow{h\nu} H_2Si(OH)_2$.

(2) Band assignments for *trans*- HSiOH, *trans*- and *cis*- HSiOD and DSiOD have been made. Force constants and thermodynamic properties have also been calculated for the *trans* isomer.

(3) A new approach has been taken to calculate the anharmonicity for the torsional mode of HSiOH ($x = 63.9$ cm^{-1}) and the SiOH bond angle ($SiOH = 114.5 \pm 6.0°$) using the Teller–Redlich product rule.

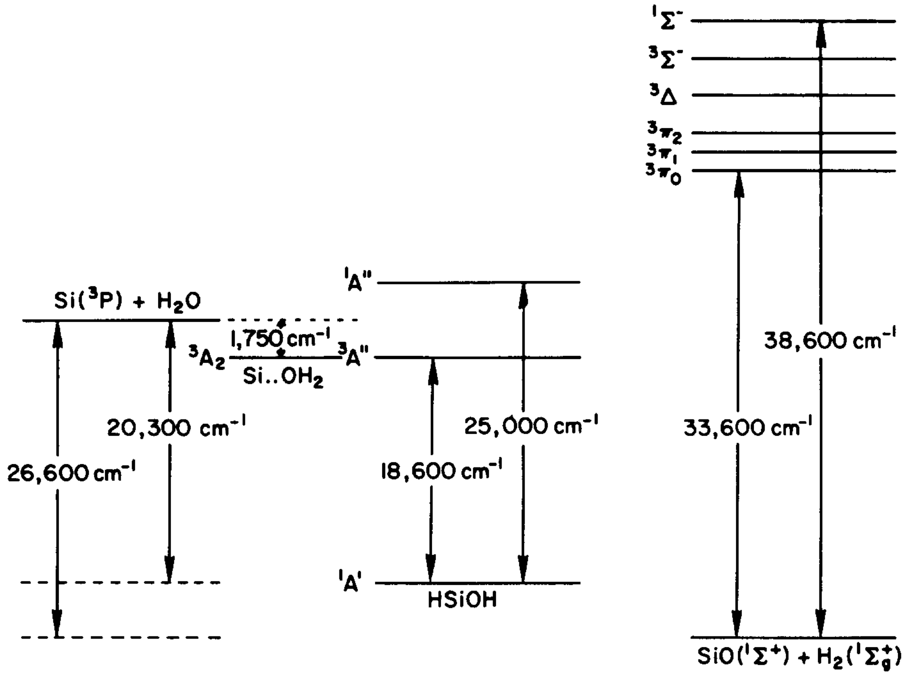

FIG. 8. Energy levels for reactants and products of the reaction of Si with H_2O.

(4) Although H_2SiO or SiO and H_2 are probably thermodynamically more stable than HSiOH, it has been possible to isolate and study this molecule by reacting Si with H_2O. This result suggests that one may be able to form and study the hydroxymethylene radical HCOH from the reaction of C atoms with water in spite of the fact that either H_2CO or H_2 and CO are much more stable.[31]

ACKNOWLEDGMENTS

This work was supported by the National Science Foundation and the Robert A. Welch Foundation. Dr. David Bonnell from the National Bureau of Standards is acknowledged for the calculations of the thermodynamic properties of HSiOH. Z. Ismail would like to acknowledge receiving partial support from a Peace Fellow ship sponsored by the U. S. AID.

[1] V. A. Nicely and J. L. Dye, J. Chem. Phys. 52, 4795 (1970).
[2] M. Trenary, H. F. Schaeffer III, and P. Kollman, J. Am. Chem. Soc. 99, 3885 (1977); J. Chem. Phys. 68, 4047 (1978).
[3] L. A. Curtiss and D. J. Frurip, Chem. Phys. Lett. 75, 69 (1980).
[4] J. D. Dill, P. R. Schleyer, J. S. Binkley, and J. A. Pople, J. Am. Chem. Soc. **99**, 6159 (1977).
[5] H. A. Kurtz and K. D. Jordan, J. Am. Chem. Soc. 102, 1177 (1980).
[6] S. Holloway and K. H. Bennemann, Surf. Sci. **101**, 327 (1980).
[7] J. Bentley, J. Am. Chem. Soc. 104, 2754 (1982).
[8] P. F. Meier, R. H. Hauge, and J. L. Margrave, J. Am. Chem. Soc. **100**, 2108 (1978).
[9] R. H. Hauge, P. F. Meier, and J. L. Margrave, Ber. Bunsenges. Phys. Chem. 82, 102 (1978).
[10] R. H. Hauge, S. E. Gransden, J. W. Kauffman, and J. L. Margrave, Proceedings of the 10th Materials Research Symposium on Characterization of High Temperature Vapors and Gases, 1979, pp. 557–567.
[11] R. H. Hauge, J. W. Kauffman, and J. L. Margrave, J. Am. Chem. Soc. **102**, 6005 (1980).
[12] P. A. Thiel, F. M. Hoffman, and W. H. Weinberg, J. Chem. Phys. **75**, 5556 (1981).
[13] J. W. Kauffman, Ph.D. thesis, Rice University, 1981.
[14] T. N. Bell, K. A. Perkins, and P. G. Perkins, J. Chem. Soc. Chem. Comm. **1980**, 1046.
[15] R. Jacquet, Kutzelnigg, and V. Staemmler, Theor. Chem. Acta Berlin **54**, 205 (1980).
[16] Z. K. Ismail, Ph.D. thesis, Rice University, 1972.
[17] D. E. Milligan and M. E. Jacox, J. Chem. Phys. **52**, 2594 (1970).
[18] L. Fredin, R. H. Hauge, Z. K. Ismail, and J. L. Margrave, (to be published).
[19] Z. K. Ismail, R. H. Hauge, L. Fredin, and J. L. Margrave, (to be published).
[20] R. R. Lembke, R. F. Ferrante, and W. Weltner Jr., J. Am. Chem. Soc. **99**, 416 (1977).
[21] K. Jordan and S. Sakai, Department of Chemistry, University of Pittsburgh (private communication).
[22] L. B. Harding, H. B. Schlegel, R. Krishnan, and J. A. Pople, J. Phys. Chem. **84**, 3394 (1980).
[23] A. D. Walsh, J. Chem. Soc. 1953, 2260.
[24] B. M. Gimarc, J. Am. Chem. Soc. **92**, 266 (1970).
[25] N. C. Craig and I. W. Levin, J. Chem. Phys. **71**, 400 (1979).
[26] R. H. Hauge, J. W. Kauffman, L. Fredin, and J. L. Margrave, ACS Symp. Ser. **179**, 370 (1982).
[27] Z. K. Ismail, L. Fredin, R. H. Hauge, and J. L. Margrave, J. Chem. Phys. **77**, 1626 (1982).
[28] J. M. Schachtsneider, Tech. Rep. Nos. 231-64 and 57-65, Shell Development Co. (1964).
[29] V. M. Khanna, R. H. Hauge, R. F. Curl, and J. L. Margrave, J. Chem. Phys. **47**, 5031 (1967).
[30] B. T. Dowling and D. M. Dennison, Phys. Rev. **57**, 128 (1940).
[31] M. J. Frisch, R. Krishnan, and J. A. Pople, J. Phys. Chem. 85, 1467 (1981).